PARALLEL LAGRANGE-NEWTON-KRYLOV-SCHUR ALGORITHMS FOR PDE-CONSTRAINED OPTIMIZATION PART II: THE LAGRANGE-NEWTON SOLVER AND ITS APPLICATION TO OPTIMAL CONTROL OF STEADY VISCOUS FLOWS*

GEORGE BIROS† AND OMAR GHATTAS‡

Abstract. In this paper we follow up our discussion on algorithms suitable for optimization of systems governed by partial differential equations. In the first part of of this paper we proposed a Lagrange-Newton-Krylov-Schur method (LNKS) that uses Krylov iterations to solve the Karush-Kuhn-Tucker system of optimality conditions, but invokes a preconditioner inspired by reduced space quasi-Newton algorithms. In the second part we focus our discussion to the outer iteration and we provide details on how to obtain a robust and globally convergent algorithm. Newton's step is known to lead to divergence for points far from the optimum. Furthermore for highly nonlinear problems the computation of a step by itself is very difficult (for both QN-RSQP and LNKS methods). As a remedy we employ line search methods, mixing quasi-Newton with Newton algorithms and continuation. We test the globalized LNKS algorithm on a optimal flow control problem were the constraints are the steady incompressible Navier-Stokes equations. The objective function is the minimization of the dissipation functional. We report results from runs on up to 128 processors on a T3E-900 at the Pittsburgh Supercomputing Center. Tests on cylinder and wing flow problems demonstrate the very good parallelism and scalability of the new method. Moreover, LNKS is an order of magnitude faster than reduced quasi-Newton SQP, and we are able to solve previously intractable problems of up to 800,000 state and 5,000 decision variables—at 5 times the cost of a single PDE solution.

1. Introduction. In the first part of the paper we concentrated on the Krylov-Schur solver–the inner iterative solver and the preconditioner that accelerate the computations of a Newton step for the KKT optimality conditions. We also examined the parallelizability and scalability of the LNKS algorithm. In the second part we follow up with algorithmic and implementation details on the outer Lagrange-Newton solver. We also look at more stringent test problems that contain many features of the most challenging PDE-constrained optimization problems: three-dimensionality, multicomponent coupling, large scale, nonlinearity, and ill-conditioning. The problem is one of optimal control of a viscous incompressible fluid by boundary velocities, a problem of both theoretical and industrial interest.

Following part I, we refer to the unknown PDE field quantities as the *state variables*; the PDE constraints as the *state equations*; solution of the PDE constraints as the *forward problem*; the inverse, design, or control variables as the *decision variables*; and the problem of determining the optimal values of the inverse, design, or control variables as the *optimization problem*.

This paper is organized as follows: In Section 2 we present our globalization methodologies. We give details on three techniques: line search, mixing QN-RSQP steps with LNKS steps, and continuation. To enhance robustness, these methodologies are combined in the globalized LNKS algorithm. We also discuss inexact Newton methods and how they fit within the context of the LNKS algorithm. Implementation specifics are given at the end of this section.

Let us add some comments on our notation conventions. We use boldface characters to denote vector valued functions and vector valued function spaces. We use roman characters

*This work is a part of the Terascale Algorithms for Optimization of Simulations (TAOS) project at CMU, with support from NASA grant NAG-1-2090, NSF grant ECS-9732301 (under the NSF/Sandia Life Cycle Engineering Program), and the Pennsylvania Infrastructure Technology Alliance. Computing services on the Pittsburgh Supercomputing Center's Cray T3E were provided under PSC grant BCS-960001P.

†Courant Institute of Mathematical Sciences, New York University, New York, NY 10012, USA (biros@cims.nyu.edu).

‡Laboratory for Mechanics, Algorithms, and Computing, Carnegie Mellon University, Pittsburgh, Pennsylvania, 15213, USA (oghattas@cs.cmu.edu).

Working paper.

to denote discretized quantities and italics for their continuous counterparts. For example $\boldsymbol{u}$ will be the continuous velocity field and $\mathbf{u}$ will be its discretization. Greek letters are overloaded and whether we refer to the discretization or the continuous fields should be clear from context. We also use $(+)$ as a subscript or superscript to denote variable updates within an iterative algorithm.

2. The Newton solver. Let us reconsider the constrained optimization problem formulation,

$$\min_{\mathbf{x}\in\mathbb{R}^N} f(\mathbf{x}) \quad \text{subject to} \quad \mathbf{c}(\mathbf{x}) = \mathbf{0}, \tag{2.1}$$

where $\mathbf{x} \in \mathbb{R}^N$ are the optimization variables, $f : \mathbb{R}^N \to \mathbb{R}$ is the objective function and $\mathbf{c} : \mathbb{R}^N \to \mathbb{R}^n$ are the constraints, which in our context are the discretized state equations. The Lagrangian,

$$\mathcal{L}(\mathbf{x}, \boldsymbol{\lambda}) := f(\mathbf{x}) + \boldsymbol{\lambda}^T \mathbf{c}(\mathbf{x}), \tag{2.2}$$

is used to convert the constrained optimization problem to a system of nonlinear equations.These equations are the first order optimality conditions:

$$\left\{ \begin{array}{c} \partial_x \mathcal{L} \\ \partial_\lambda \mathcal{L} \end{array} \right\} (\mathbf{x}, \boldsymbol{\lambda}) = \left\{ \begin{array}{c} \mathbf{g}(\mathbf{x}) + \mathbf{A}(\mathbf{x})^T \boldsymbol{\lambda} \\ \mathbf{c}(\mathbf{x}) \end{array} \right\} = \mathbf{0} \quad (\text{or } \mathbf{h}(\mathbf{q}) = \mathbf{0}). \tag{2.3}$$

We use $\mathbf{g}$ for the gradient of the objective function, $\mathbf{A}$ for the Jacobian of the constraints and $\mathbf{W}$ for the Hessian of the Lagrangian. We use Newton's method to solve for $\mathbf{x}$ and λ. A Newton step on the optimality conditions is given by

$$\left[\begin{array}{cc} \mathbf{W} & \mathbf{A}^T \\ \mathbf{A} & \mathbf{0} \end{array} \right] \left\{ \begin{array}{c} \mathbf{p}_x \\ \mathbf{p}_\lambda \end{array} \right\} = - \left\{ \begin{array}{c} \mathbf{g} + \mathbf{A}^T \boldsymbol{\lambda} \\ \mathbf{c} \end{array} \right\} \quad (\text{ or } \mathbf{K}\mathbf{v} = -\mathbf{h}), \tag{2.4}$$

where $\mathbf{p}_x$ and $\mathbf{p}_\lambda$ are the updates of $\mathbf{x}$ and $\boldsymbol{\lambda}$ from current to next iterations. In Part I we reviewed the most popular algorithm for solving for a KKT point, the RSQP algorithm and its quasi-Newton variant (Algorithm 3 in the first paper). Although these algorithms are very efficient and robust, they do not scale very well with the number of decision variables. These algorithms avoid solving (2.4) directly, but require a large number of linearized forward solves and thus can be inefficient for large-scale PDE-constrained optimization. We argued that a better approach would be to stay in the full space and use a Krylov method to solve (2.4). However, the KKT matrix is notoriously ill-conditioned. In the first part of this paper we addressed this problem by proposing efficient preconditioning techniques. The key idea was to use approximate versions of QN-RSQP as preconditioners. We showed that RSQP can be viewed as a block-LU factorization in which the reduced Hessian $\mathbf{W}_z$ is the Schur complement for the decision variables and this forms the basis of the preconditioner. The basic sketch of the LNKS algorithm given by Algorithm 1. We termed the method "Lagrange-Newton-Krylov-Schur", algorithm for concatenation of "Lagrange-Newton" method which is used in the outer iteration and "Krylov-Schur" is used to converge the inner iteration. We also provided theoritical and numerical evidence that these preconditioners work very well. In order to isolate the inner iteration we solved problems with quadratic objective functions and linear constraints (quadratic programs).

Nevertheless, there are two questions that should be answered before we can claim a fast and robust general-purpose algorithm. The first one is whether LNKS algorithm is convergent for any initial guess $(\mathbf{x}_0, \boldsymbol{\lambda}_0)$ and the second is whether we can utilize inexact[1] Newton methods to further accelerate LNKS. Within this framework we examine line search algorithms, mixing QN-RSQP and LNKS algorithms, continuation, and inexact Newton methods.

[1] Some authors use the term "truncated" instead of "inexact".

Algorithm 1 Lagrange-Newton-Krylov-Schur

1: Choose $\mathbf{x}, \boldsymbol{\lambda}$
2: **loop**
3: Check for convergence
4: Compute $\mathbf{c}, \mathbf{g}, \mathbf{A}, \mathbf{W}$
5: Solve $\mathbf{P}^{-1}\mathbf{K}\mathbf{v} = \mathbf{P}^{-1}\mathbf{h}$ (Newton Step)
6: Update $\mathbf{x} = \mathbf{x} + \mathbf{p}_x$
7: Update $\boldsymbol{\lambda} = \boldsymbol{\lambda} + \mathbf{p}_\lambda$
8: **end loop**

3. Line search methods. Algorithm 1 is only locally convergent. Popular methodologies to globalize Newton's method include line search and trust region algorithms. Details can be found in [18]. Recently, there has been an increased interest in trust region methodologies, especially in combination with RSQP and inexact Newton methods. These methods have been successfully applied to PDE-constrained optimization [11], [14], [16]. Global convergence proofs for these methods can be found in [3]. Trust region methods are based on the Steihaug modification [21] of the Conjugate Gradient (CG) algorithm. However, this approach works only with positive definite systems. Since the reduced Hessian is assumed to be positive definite CG can be used. It is not obvious how to use trust-regions with an indefinite Krylov solver (which is required for the KKT system) and thus we have opted to use a line search algorithm.

The basic component of a line search algorithm is the choice of a merit function; a scalar function (of the optimization variables) that monitors the progress of the algorithm. In contrast with unconstrained optimization, the choice of a merit function is not straightforward since we are trying to balance minimization of the objective function with feasibility. The two most popular choices are the l_1-merit function and the augmented Lagrangian. The l_1-merit function is given by

$$\phi(\mathbf{x}) := f + \rho_\phi \|\mathbf{c}\|_1, \tag{3.1}$$

and augmented Lagrangian by

$$\phi(\mathbf{x}, \boldsymbol{\lambda}) := f + \mathbf{c}^T\boldsymbol{\lambda} + \frac{\rho_\phi}{2}\mathbf{c}^T\mathbf{c}. \tag{3.2}$$

The scalar ρ_ϕ is the *penalty parameter*—a weight chosen to bring the right balance between minimizing the objective function and minimizing the residuals of the constraints. Both merit functions are exact provided the penalty parameter is large enough. By exact we mean that if $(\mathbf{x}_*, \boldsymbol{\lambda}_*)$ is a minimizer for (2.1), then it is also an (unconstrained) minimizer for the merit function. A crucial property of a merit function is that it should accept unit step lengths close to a solution, and therefore permit Newton quadratic convergence to be observed. The l_1-merit function often suffers from the "Maratos" effect, that is, sometimes it rejects good steps and slows down the algorithm. The augmented Lagrangian merit function does not exhibit such behavior but its drawback is that it requires accurate estimates of the Lagrange multipliers to perform well. Both algorithms are sensitive to the penalty parameter which must be judiciously chosen; otherwise, it can result in an unbounded merit function, or very slow algorithms.

The outline of the algorithm for a line search based optimization is given in Algorithm 2. We use $\phi(0)$ for $\phi(\mathbf{q})$ and $\phi(\alpha)$ for $\phi(\mathbf{q} + \alpha\mathbf{v})$ (likewise for the derivative $\nabla\phi$). The algorithm used to compute the search direction $\mathbf{v}$ is left intentionally unspecified. All that

Algorithm 2 Line search

1: Choose $\mathbf{q}$, $\delta_A > 0$ and κ_1, κ_2 arbitrary constants
2: **while** Not converged **do**
3: Compute search direction $\mathbf{v}$ so that
$\mathbf{v}^T \nabla\phi(0) < 0$
$|\ \mathbf{v}^T \nabla\phi(0)| \geq \kappa_1 \|\mathbf{v}\|\, \|\nabla\phi(0)\|$
$\|\mathbf{v}\| \geq \kappa_2 \|\nabla\phi(0)\|$
4: Compute α such that $\phi(\alpha) \leq \phi(0) + \alpha\delta_A \mathbf{v}^T \nabla\phi(0)$ Armijo criterion
5: Set $\mathbf{q} = \mathbf{q} + \alpha\mathbf{v}$
6: **end while**

matters to ensure global convergence, is the properties of the merit function and the properties of $\mathbf{v}$. The conditions 3 in Algorithm 2 are descent direction, sufficient angle and sufficient step size conditions [7]. The condition in Step 4 is often called the Armijo condition. If ϕ is bounded and takes its minimum at a finite point, and if $\mathbf{v}$ is bounded, Algorithm 2 is guaranteed to converge to a local minimum if search directions are bounded [17]. The line search algorithm we use is simple backtracking (with a factor of 0.5). The search is bounded so that $\alpha_{min} \leq \alpha \leq 1$. As mentioned before, the choice of the penalty parameter has a great effect on the performance of the algorithm.

For the l_1-merit function the update is relatively straightforward. The directional derivative for a search direction $\mathbf{p}_x$ is given by

$$\nabla\phi^T \mathbf{p}_x = \mathbf{g}^T \mathbf{p}_x - \rho_\phi \|\mathbf{c}\|_1. \tag{3.3}$$

If $\mathbf{W}_z$ is positive definite it can be shown that by setting

$$\rho_\phi = \|\boldsymbol{\lambda}\|_\infty + \delta, \quad \delta > 0, \tag{3.4}$$

we obtain a descent direction. In numerical experiments the l_1-merit function performed reasonably well. However, we did observe the Maratos effect, usually on steps computed by QN-RSQP. To overcome this obstacle we have implemented the second order correction trick (used only with QN-RSQP), in which an extra normal step (towards feasibility) is taken ([18], p.570).

When an augmented Lagrangian merit function is used the penalty parameter should be chosen differently. The inclusion of Lagrange multipliers slightly complicates the algorithm. Some researchers consider $\boldsymbol{\lambda}$ as a function of $\mathbf{x}$ [2], [6], but others treat it as an independent variable [3], [20]. In [22] the derivative of the merit with respect to $\boldsymbol{\lambda}$ is taken to be zero. The directional derivative of the augmented Lagrangian merit function is given by

$$\nabla\phi^T \mathbf{v} = (\mathbf{g} + \mathbf{A}^T\boldsymbol{\lambda} + \rho_\phi \mathbf{A}^T\mathbf{c})^T \mathbf{p}_x + \mathbf{c}^T \mathbf{p}_\lambda. \tag{3.5}$$

In LNKS we solve for $\boldsymbol{\lambda}$ simultaneously with $\mathbf{x}$ and it is natural to use the step $\mathbf{p}_\lambda$. On the other hand, QN-RSQP uses $\boldsymbol{\lambda} = -\mathbf{A}_s^{-T}\mathbf{g}_s$ and it seems natural to consider $\boldsymbol{\lambda}$ a function of $\mathbf{x}$. In this case the last term in (3.5) is given by

$$\mathbf{c}^T \mathbf{p}_\lambda = \mathbf{c}^T (\partial_x \boldsymbol{\lambda}) \mathbf{p}_x,$$

where

$$\partial_x \boldsymbol{\lambda} := -\mathbf{A}_s^{-T} \begin{bmatrix} \mathbf{W}_{ss} & \mathbf{W}_{sd} \end{bmatrix}.$$

If we set

$$\rho_\phi = \frac{(\mathbf{g} + \mathbf{A}^T\boldsymbol{\lambda})\mathbf{p}_x + \mathbf{c}^T\mathbf{p}_\lambda + \delta}{\mathbf{c}^T\mathbf{A}\mathbf{p}_x}, \quad \delta > 0, \tag{3.6}$$

we obtain a descent direction.

4. Combining QN-RSQP with LNKS. For iterates far from the solution, relying solely on a line search algorithm will not work since the Newton step is likely to be of very poor quality. Usually global convergence can be shown if the reduced Hessian ($\mathbf{W}_z$) is positive definite (and not the full Hessian $\mathbf{W}$). If $\mathbf{W}_z$ is positive definite (and assuming the system (2.4) is solved exactly), then the resulting step $\mathbf{v}$ satisfies the descent criterion (for reasonable merit functions.). This is where quasi-Newton methods have an advantage over Newton methods. For example, by using a BFGS approximation of $\mathbf{W}_z$, positive definiteness can be guaranteed. LNKS does maintain a BFGS approximation—not for driving the outer iteration but for preconditioning purposes. Therefore, the remedy for an indefinite reduced Hessian is simple: if a computed search direction fails to satisfy the test of the line search algorithm, we discard the search directions and take a QN-RSQP step. For this reason, even if we use a different preconditioner for the reduced Hessian, we also maintain a BFGS approximation of $\mathbf{W}_z$.

5. Continuation. One of the standard assumptions in global convergence proofs is that the Jacobian of the constraints is non-singular for all iterates of the optimization variables. For highly nonlinear PDEs like the Navier-Stokes equations this is an unrealistic assumption. Even if the Jacobian is nonsingular, severe ill-conditioning will cause both QN-RSQP and LNKS algorithms to stall. Indeed, in our numerical experiments the most difficult challenge (for iterates far from the solution) was converging the $\mathbf{A}_s$ or $\mathbf{K}$ linear solves. Krylov solvers reached their maximum iteration bounds with the (linear system) residuals not having decreased significantly. As a result, the iterates were of very poor quality and the algorithm stagnated as it was impossible to compute a search direction, be it from QN-RSQP or LNKS.

A remedy to this problem is continuation. This idea (in its simplest form) works when we can express the nonlinearity of the problem as a function of a single scalar parameter. Continuation is particularly suitable for PDE-constrained optimization because it is quite typical for a PDE to have a parameter that scales the nonlinearities. Examples of such parameters are the Reynolds and Mach numbers in fluid mechanics, the Peclet number in general convection diffusion equations, and the Hartman number in magnetohydrodynamics. In problems where such a parameter cannot be found an alternative is pseudo-transient continuation [15].

Continuation allows uphill steps (unlike monotone line search methods) to be taken and generates good initial guesses, not only for the optimization variables, but also for the penalty parameter in the merit function. The most important feature of the continuation algorithm is that it globalizes trivially[2]. If the continuation step brings the next iterate outside the attraction basin of the Newton method the we simply reduced the step size. In principle, the method can be made to work without incorporating any other globalization strategy. Nevertheless, taking a large number of continuation steps can significantly slow down the algorithm. Experience from our numerical experiments suggests that the best strategy is a combination of line searching, QN steps for indefinite Hessians, and continuation.

6. Inexact Newton's method. Before we discuss inexact Newton's method in the context of LNKS, we briefly summarize a few results for a general nonlinear system of equations.

[2]This is true only when all iterates on the continuation path are far from turning and bifurcation points. In other words, the physics of the problem does not produce singular Jacobians.

Assume we want to solve $\mathbf{h}(\mathbf{q}) = \mathbf{0}$. Further assume the following: (1) $\mathbf{h}$ and $\mathbf{K} := \partial_q \mathbf{h}$ are smooth enough in a neighborhood of a solution $\mathbf{q}_*$; (2) at each iteration an inexact Newton method computes a step $\mathbf{v}$ that satisfies

$$\|\mathbf{K}\mathbf{v} + \mathbf{h}\| \leq \eta_N \|\mathbf{h}\|, \tag{6.1}$$

where η_N is often called the *forcing term*. It can be shown that if $\eta_N < 1$ then $\mathbf{q} \to \mathbf{q}^*$ linearly; if $\eta_N \to 0$ then $\mathbf{q} \to \mathbf{q}^*$ superlinearly; and if $\eta_N = \mathcal{O}(\|\mathbf{h}\|)$ then we recover the quadratic convergence rates of a Newton method. The forcing term is usually given by

$$\eta_N = \frac{\|\mathbf{h}_{(+)} - \mathbf{h} - \mathbf{K}\mathbf{v}\|}{\|\mathbf{h}\|}. \tag{6.2}$$

Other alternatives exist (for details see [5]).

The extension of inexact methods to optimization is immediate, especially for unconstrained optimization. In [11] a global analysis is provided for a trust region RSQP-based algorithm. Close to a KKT point the theory for Newton's method applies and one can use the analysis presented in [4] to show that the inexact version of the LNKS algorithm converges. However, the line search we are using is not based on the residual of the KKT equations but instead on the merit function discussed in the previous session. That means that an inexact step that simply reduces $\mathbf{h}$ may not satisfy the merit function criteria. We will next show that for points close enough to the solution inexactness does not interfere with the line search. In our analysis we use the augmented Lagrangian merit function.We assume that, locally, $\mathbf{A}$ and $\mathbf{K}$ are non-singular and uniformly bounded. We define $\kappa_1 := \max\|\mathbf{K}^{-1}(\mathbf{q})\|$ for $\mathbf{q}$ in the neighborhood of the solution $\mathbf{q}_*$. We also define $\mathbf{v}$ as the exact solution of the (linearized) KKT system so that

$$\mathbf{K}\mathbf{v} + \mathbf{h} = \mathbf{0},$$

and $\tilde{\mathbf{v}}$ the approximate solution so that

$$\mathbf{K}\tilde{\mathbf{v}} + \mathbf{h} = \mathbf{r}.$$

We also have $\|\mathbf{r}\| = \eta_N \|\mathbf{h}\|$ from the inexact Newton stopping criterion (6.1). By (2.3) we get that $\|\mathbf{h}\|^2 = \|\mathbf{g} + \mathbf{A}^T\boldsymbol{\lambda}\|^2 + \|\mathbf{c}\|^2$ and since $\mathbf{A}$ is bounded, there is constant κ_2 such that:

$$\|\mathbf{A}^T\mathbf{c}\| \leq \kappa_2 \|\mathbf{h}\|. \tag{6.3}$$

We assume the following: (1) ρ_ϕ is sufficiently large so that the merit function is exact and $\|\nabla\phi\| \geq \kappa_3\|\mathbf{h}\|$ for some constant κ_3; (2) $\mathbf{v}$ satisfies the gradient and length conditions, as well as the Armijo condition. From the latter it is immediate that $\mathbf{v}$ satisfies the Cauchy fraction condition[3]:

$$|\nabla\phi^T\mathbf{v}| \geq 2\kappa_4 \|\nabla\phi\|^2. \tag{6.4}$$

We will show that if η_N is small enough then the approximate step $\tilde{\mathbf{v}}$ satisfies the Cauchy fraction condition, and that it satisfies the gradient and length conditions. Then, we will use a theorem from [17] to conclude that the Armijo condition is satisfied with unit steplengths and thus if $\eta_N = \mathcal{O}(\|\mathbf{h}\|)$ quadratic convergence is preserved.

Note that

$$\nabla\phi^T\tilde{\mathbf{v}} = \nabla\phi^T\mathbf{v} + \nabla\phi^T\mathbf{K}^{-1}\mathbf{r}$$

[3]The Cauchy step is a steepest descent step for the merit function.

and thus by (6.4) we get

$$|\nabla\phi^T\tilde{\mathbf{v}}| \geq 2\kappa_4\|\nabla\phi\|^2 - |\nabla\phi^T\mathbf{K}^{-1}\mathbf{r}|$$

Therefore to satisfy the Cauchy fraction condition

$$|\nabla\phi^T\tilde{\mathbf{v}}| \geq \kappa_4\|\nabla\phi\|^2, \tag{6.5}$$

we need to show that

$$|\nabla\phi^T\mathbf{K}^{-1}\mathbf{r}| \leq \kappa_4\|\nabla\phi\|^2. \tag{6.6}$$

The gradient of the merit function is given by

$$\nabla\phi = \mathbf{h} + \rho_\phi \begin{Bmatrix} \mathbf{A}^T\mathbf{c} \\ \mathbf{0} \end{Bmatrix},$$

and thus

$$\begin{aligned}
|\nabla\phi^T\mathbf{K}^{-1}\mathbf{r}| &= |\mathbf{h}^T\mathbf{K}^{-1}\mathbf{r} + \rho_\phi \begin{Bmatrix} \mathbf{A}^T\mathbf{c} \\ \mathbf{0} \end{Bmatrix}^T \mathbf{K}^{-1}\mathbf{r}| \\
&\leq \kappa_1 \left(\|\mathbf{h}\|\,\|\mathbf{r}\| + \rho_\phi\|\mathbf{A}^T\mathbf{c}\|\,\|\mathbf{r}\|\right) \\
&\leq \kappa_1\eta_N \left(\|\mathbf{h}\|^2 + \rho_\phi\|\mathbf{A}^T\mathbf{c}\|\,\|\mathbf{h}\|\right) \\
&\leq \kappa_1\eta_N(1+\rho_\phi\kappa_2)\|\mathbf{h}\|^2 \\
&\leq \kappa_1\eta_N(1+\rho_\phi\kappa_2)\frac{\|\nabla\phi\|^2}{\kappa_3^2}
\end{aligned}$$

If

$$\eta_N \leq \frac{\kappa_4\,\kappa_3^2}{\kappa_1(1+\rho_\phi\kappa_2)} \tag{6.7}$$

then (6.6) holds. If we choose a superlinearly convergent inexact Newton variant then

$$\eta_N \to 0,$$

and therefore close to the solution (6.7) is satisfied. We also have that

$$\begin{aligned}
\tilde{\mathbf{v}} &= \mathbf{K}^{-1}(\mathbf{r}-\mathbf{h}) \\
\|\tilde{\mathbf{v}}\| &\leq \kappa_1(1+\eta_N)\|\mathbf{h}\| \\
\|\tilde{\mathbf{v}}\| &\leq \kappa_1(1+\eta_N)\frac{\|\nabla\phi\|}{\kappa_3}. \qquad (6.8)
\end{aligned}$$

By combining (6.8) and (6.5) we get

$$|\nabla\phi^T\tilde{\mathbf{v}}| \geq \|\nabla\phi\|^2 \geq \|\nabla\phi\|\,\|\tilde{\mathbf{v}}\|,$$

and

$$\begin{gathered}
\|\nabla\phi\|\,\|\tilde{\mathbf{v}}\| \geq |\nabla\phi^T\tilde{\mathbf{v}}| \geq \|\nabla\phi\|^2 \;\Rightarrow \\
\|\tilde{\mathbf{v}}\| \geq \|\nabla\phi\|.
\end{gathered}$$

That is, the gradient and angle conditions are satisfied. It can be shown ([17], Theorem 10.6) that the Armijo condition can be satisfied with α bounded below, and thus by choosing δ_A small enough, the Armijo condition is satisfied with unit steplength. Hence the quadratic convergence rates associated with Newton's method are observed, i.e. the inexactness does not interfere with the merit function. In addition it can be shown that the augmented Lagrangian merit function allows unit steplength near the solution (see [6], [20] and the references therein). Finally, notice that convergence does not require that $\eta_N \to 0$; it only requires that η_N is small enough. This is in contrast with inexact reduced space methods which require the tolerances to tighten as the iterates approach the solution (reduced gradient needs to be computed accurately.).

7. The globalized LNKS algorithm. In the previous sections we discussed the various features of our globalization strategies. In this section we summarize by giving a high-level description of implementation details and heuristics we are using in the globalized LNKS. The statement of the algorithm is given by Algorithm 3. The algorithm uses a three-level iter-

Algorithm 3 Globalized LNKS

1: Choose $\mathbf{x}_s,\ \mathbf{x}_d,\ \rho_\phi,\ t,\ \delta_A$, set $Re = Re_{start},\ tol = tol_0$
2: $\mathbf{A}_s^T\boldsymbol{\lambda} + \mathbf{g}_s \approx \mathbf{0}$ — solve inexactly for $\boldsymbol{\lambda}$
3: **while** $Re \neq Re_{target}$ **do**
4: **loop**
5: Evaluate $f,\ \mathbf{c},\ \mathbf{g},\ \mathbf{A},\ \mathbf{W}$
6: $\mathbf{g}_z = \mathbf{g}_d + \mathbf{A}_d^T\boldsymbol{\lambda}$
7: Check convergence: $\|\mathbf{g} + \mathbf{A}^T\boldsymbol{\lambda}\| \leq tol$ and $\|\mathbf{c}\| \leq tol$
8: $\mathbf{P}^{-1}\mathbf{K}\mathbf{v} + \mathbf{P}^{-1}\mathbf{h} \approx \mathbf{0}$ — solve inexactly for $\mathbf{v}$
9: Compute ρ_ϕ such that $\nabla\phi^T(0)\mathbf{v} \leq 0$
10: Compute α s.t. $\phi(\alpha) \leq \phi(0) + \delta_A\alpha(\nabla\phi^T(0)\mathbf{v})$
11: **if** Line search failed **then**
12: Compute α s.t. $\|\mathbf{h}(\alpha)\|^2 < t\|\mathbf{h}(0)\|^2$
13: **end if**
14: **if** LNKS step failed **then**
15: $\mathbf{B}_z\mathbf{p}_d = -\mathbf{g}_z$ — solve inexactly for $\mathbf{p}_d$
16: $\mathbf{A}_s\mathbf{p}_s + \mathbf{A}_d\mathbf{p}_d + \mathbf{c} \approx \mathbf{0}$ — solve inexactly for $\mathbf{p}_s$
17: $\mathbf{A}_s^T\boldsymbol{\lambda}_+ + \mathbf{g}_s \approx \mathbf{0}$ — solve inexactly for $\boldsymbol{\lambda}_+$
18: Compute α s.t. $\phi(\alpha) \leq \phi(0) + \delta_A\alpha(\nabla\phi^T(0)\mathbf{v})$
19: **if** Line search on QN-RSQP step failed **then**
20: Reduce Re and go to step 5.
21: **end if**
22: **end if**
23: $\boldsymbol{\lambda}_+ = \boldsymbol{\lambda} + \mathbf{p}_\lambda$ — (only for LNKS step)
24: $\mathbf{x}_+ = \mathbf{x} + \mathbf{p}_x$
25: **end loop**
26: $Re = Re + \Delta Re$
27: Tighten tol
28: **end while**

ation. In the outer iteration the continuation parameter number is gradually increased until the target number is reached.The middle iterations correspond to Lagrange-Newton linearizations of the optimality system for a fixed continuation number. Finally, the inner iteration consists of two core branches: the computation of an LNKS search direction and the computation of

the search direction with QN-RSQP. The default branch is the LNKS step. If this step fails to satisfy the line search algorithm conditions then we switch to QN-RSQP. If QN-RSQP fails too, then we reduce the continuation parameter Re and we return to the outer loop.

Here we clarify some specific features of the algorithm:

- Linear solves at steps 8, 16 and 17 are performed inexactly. We follow [5] in choosing the forcing term. In steps 16, and 17 the forcing term formula uses $\|\mathbf{c}\|$, whereas in 8 it uses $\|\mathbf{h}\|$. In 7 we also used $\|\nabla\phi\|$ but in numerical experiments we found no significant differences.
- In step 6 we use the adjoint variables to update the reduced gradient. This is equivalent to $\mathbf{g}_z = \mathbf{g}_d - \mathbf{A}_d^T \mathbf{A}_s^{-T} \mathbf{g}_s$, if $\boldsymbol{\lambda}$ is computed by solving exactly $\mathbf{A}_s^T \boldsymbol{\lambda} + \mathbf{g}_s = \mathbf{0}$. When $\boldsymbol{\lambda}$ is taken from LNKS, it includes second order terms (which reduce to zero as we approach the solution), and when $\boldsymbol{\lambda}$ is taken from QN-RSQP it also introduces extra error since we never solve the linear systems exactly. In our numerical experiments this approximation has not caused problems.
- We use various heuristics to bound the penalty parameter and if possible reduce it. A new penalty parameter ρ_ϕ^+ is computed using the LNKS step and formula (3.6). If $\rho_\phi^+ > 4\rho_\phi$ we update the penalty parameter and we switch to QN-RSQP. If $\rho_\phi^+ < 4\rho_\phi$ we *reduce* the penalty parameter and set $\rho_\phi^+ = 0.5\rho_\phi$. We also use the augemented Lagrangian merit when we evaluate QN-RSQP steps. Another alternative would be to use the l_1-merit function.
- We allow for non-monotone line searches. If the LNKS step is rejected by the merit function line search we do not switch immediately to QN-RSQP. Instead we do a line search (step 12) on the KKT residual (as if we were treating the KKT conditions as nonlinear equations) and if the step is accepted we use it to update the variables for the next iteration. However, we do store the iterate and the merit function gradient, and we insist that some step satisfies the conditions of the merit line search (evaluated at the failure point) after a fixed number of iterations. Otherwise, we switch to QN-RSQP. This heuristic has been very successful. Typically, we permit two steps before we demand reduction of the merit function.

Algorithm 4 Limited BFGS

1: $\mathbf{q} = \mathbf{x}$, and $l =$ number of stored vectors
2: **for** $i = k-1, k-2, \ldots, k-l$ **do**
3: $\quad \alpha_i = \omega_i \, \mathbf{s}_i^T \mathbf{q}$
4: $\quad \mathbf{q} = \mathbf{q} - \alpha_i \mathbf{y}_i$
5: **end for**
6: $\mathbf{z} = \mathbf{B}_{z,0}^{-1} \mathbf{q}$
7: **for** $i = k-l, k-l+1, \ldots, k-1$ **do**
8: $\quad \beta = \omega_i \, \mathbf{y}_i^T \mathbf{z}$
9: $\quad \mathbf{z} = \mathbf{z} + \mathbf{s}_i(\alpha_i - \beta)$
10: **end for**

- We use the BFGS method for the quasi-Newton approximation of the reduced Hessian. The name comes from the inventors of the method, Broyden, Fletcher, Goldfarb, and Shanno. At each outer iteration we compute

$$\mathbf{s} = \mathbf{p}_d^{(+)} - \mathbf{p}_d,$$
$$\mathbf{y} = \mathbf{g}_z^{(+)} - \mathbf{g}_z,$$

and the update of the approximation to the inverse of the reduced Hessian is given by

$$\mathbf{B}_+^{-1} = (I - \omega \mathbf{y}\mathbf{s}^T)^T \mathbf{B}^{-1} (I - \omega \mathbf{y}\mathbf{s}^T) + \omega \mathbf{s}\mathbf{s}^T, \;\; \omega = \frac{1}{\mathbf{y}^T \mathbf{s}}. \tag{7.1}$$

If we encounter an iterate that has $\mathbf{y}^T\mathbf{s} \leq \kappa \|\mathbf{y}\|$ we skip the update. $\mathbf{B}^{-1}$ is dense; thus for large decision-space problems, storing this matrix (or a factorization of it) can be problematic or even impossible. Furthermore, it is not obvious how to parallelize the application of a dense $\mathbf{B}^{-1}$ to a vector since it involves all-to-all communication and may be very expensive on a parallel computer. For these reasons we have opted for a limited memory version of the BFGS algorithm. When updating we do not compute (7.1) but instead we simply store $\mathbf{s}$ and $\mathbf{y}$. Then the action of $\mathbf{B}^{-1}$ to a vector $\mathbf{x}$ is given in Algorithm 4. Analysis and details for the convergence properties of this algorithm can be found in [18]. The stationary preconditioner can be combined with BFGS (used as $\mathbf{B}_{z,0}$).

- A Lanzos algorithm can be used to (approximately) check the second-order optimality conditions. If the lowest eigenvalue of $\tilde{\mathbf{W}}_z$ is negative then a QN-RSQP step is taken without computing the full-space directions. The eigenvalues are frozen through a single continuation step, but if a negative direction is detected they are recomputed at each SQP iteration.

In the next section we study an optimal control problem of the steady incompressible Navier-Stokes equations. We cite results on the existence and uniqueness of solutions and make comparisons between the discrete and continuous forms of the optimality conditions.

8. Formulation of an Optimal Control Problem. In this section we would like to turn our attention to the formulation and well-posedness of a specific optimization problem: the Dirichlet control of the steady incompressible Navier-Stokes equations. We present the continuous form of the Karush-Kuhn-Tucker optimality conditions and we cite convergence results for finite element approximations from [12] and [13]. A survey and articles on this topic can be found in [9]. More on the Navier-Stokes equations can be found in [8, 10]. We are studying problems in which we specify both Dirichlet and Neumann boundary conditions. The controls are restricted to be only of Dirichlet type but the theory is similar for distributed and Neumann controls.

We use the velocity-pressure $(\boldsymbol{u}, p)$ form of the incompressible steady state Navier-Stokes equations. We begin by writing a strong form of the Navier-Stokes equations:

$$\begin{aligned}
-\nu \nabla \cdot (\nabla \boldsymbol{u} + \nabla \boldsymbol{u}^T) + (\nabla \boldsymbol{u})\boldsymbol{u} + \nabla p &= \boldsymbol{b} \quad \text{in} \quad \Omega, \\
\nabla \cdot \boldsymbol{u} &= 0 \quad \text{in} \quad \Omega, \\
\boldsymbol{u} &= \boldsymbol{u}_g \quad \text{on} \quad \Gamma_u, \\
\boldsymbol{u} &= \boldsymbol{u}_d \quad \text{on} \quad \Gamma_d, \\
-p\boldsymbol{n} + \nu(\nabla \boldsymbol{u} + \nabla \boldsymbol{u}^T)\boldsymbol{n} &= \boldsymbol{0} \quad \text{on} \quad \Gamma_N.
\end{aligned} \tag{8.1}$$

Here $\nu = 1/Re$ and the decision variables are the velocities $\mathbf{u}_d$ on Γ_d. For a forward solve we need not distinguish between Γ_d and Γ_u. In the optimization problem however, $\boldsymbol{u}_d$ is not known. We will present a mixed formulation that treats the tractions on the Dirichlet boundary Γ_d as additional unknown variables. The traction variables are used to enforce the Dirichlet boundary conditions [1].

With $L^2(\Omega)$ we denote the space of scalar functions (in Ω) which are square-integrable and with $\boldsymbol{H}^1(\Omega)$ we denote vector functions whose first derivatives are in $L^2(\Omega)$. $\boldsymbol{H}^{1/2}(\Gamma)$ is the trace space (the restriction on Γ) of functions belonging to $\boldsymbol{H}^1(\Omega)$. Finally $\boldsymbol{H}^{-k}(D)$

is the set of bounded linear functionals on functions belonging to $\boldsymbol{H}^k(D)$, where D is some smooth domain in $\mathbb{R}^3$. We also define

$$\boldsymbol{V} := \left\{ \boldsymbol{v} \in \boldsymbol{H}^1(\Omega) : \boldsymbol{v}|_{\Gamma_u} = \boldsymbol{0} \right\}.$$

We define the following bilinear and trilinear forms associated with the Navier-Stokes equations:

$$\begin{aligned} a(\boldsymbol{u}, \boldsymbol{v}) &:= \int_\Omega (\nabla \boldsymbol{u} + \nabla \boldsymbol{u}^T) \cdot (\nabla \boldsymbol{v} + \nabla \boldsymbol{v}^T)\, d\Omega \quad \forall\, \boldsymbol{u}, \boldsymbol{v} \in \boldsymbol{H}^1(\Omega), \\ c(\boldsymbol{w}, \boldsymbol{u}, \boldsymbol{v}) &:= \int_\Omega (\nabla \boldsymbol{u})\boldsymbol{w} \cdot \boldsymbol{v}\, d\Omega \quad \forall\, \boldsymbol{u}, \boldsymbol{v}, \boldsymbol{w} \in \boldsymbol{H}^1(\Omega), \\ b(q, \boldsymbol{v}) &:= \int_\Omega -q \nabla \cdot \boldsymbol{v}\, d\Omega \quad \forall\, q \in L,\ \boldsymbol{v} \in \boldsymbol{H}^1(\Omega). \end{aligned}$$

We also use the notation $(\boldsymbol{x}, \boldsymbol{y})_D$ for $\int_D \boldsymbol{x} \cdot \boldsymbol{y}\, dD$.

In the weak formulation of (8.1) we seek $\boldsymbol{u} \in \boldsymbol{H}^1(\Omega),\ p \in L^2(\Omega)$ and $\boldsymbol{\sigma} \in H^{-1/2}(\Gamma_d)$ such that:

$$\begin{aligned} \nu a(\boldsymbol{u}, \boldsymbol{v}) + c(\boldsymbol{u}, \boldsymbol{u}, \boldsymbol{v}) + b(p, \boldsymbol{v}) - (\boldsymbol{\sigma}, \boldsymbol{v})_{\Gamma_d} &= (\boldsymbol{f}, \boldsymbol{v})_\Omega && \forall\, \boldsymbol{v} \in \boldsymbol{V}, \\ b(q, \boldsymbol{u}) &= 0 && \forall\, q \in L^2(\Omega), \\ -(\boldsymbol{t}, \boldsymbol{u})_{\Gamma_d} &= -(\boldsymbol{t}, \boldsymbol{u}_d)_{\Gamma_d} && \forall\, \boldsymbol{t} \in \boldsymbol{H}^{-1/2}(\Gamma_d). \end{aligned} \tag{8.2}$$

We also define $\boldsymbol{d}$ to be the decision field (so that $\boldsymbol{u}_d = \boldsymbol{d}$). Based on the above formulation we can proceed in defining the Lagrangian function for the optimization problem. The objective function is given by

$$\mathcal{J}(\boldsymbol{u}, \boldsymbol{d}) := \frac{\nu}{2} a(\boldsymbol{u}, \boldsymbol{u}) + \frac{\rho}{2} (\boldsymbol{d}, \boldsymbol{d})_{\Gamma_d},$$

and (the weak form of) the constraints are given by (8.2). We define the Lagrangian function as follows:

$$\begin{aligned} \mathcal{L}(\boldsymbol{u}, p, \boldsymbol{d}, \boldsymbol{\sigma}, \boldsymbol{\lambda}, \mu, \boldsymbol{\tau}) &:= \mathcal{J}(\boldsymbol{u}, \boldsymbol{d}) \\ &\quad + \nu a(\boldsymbol{u}, \boldsymbol{\lambda}) + c(\boldsymbol{u}, \boldsymbol{u}, \boldsymbol{\lambda}) - (\boldsymbol{\sigma}, \boldsymbol{\lambda})_{\Gamma_d} - (\boldsymbol{f}, \boldsymbol{\lambda})_\Omega + b(p, \boldsymbol{\lambda}) \\ &\quad + b(\mu, \boldsymbol{u}) - (\boldsymbol{\tau}, \boldsymbol{u} - \boldsymbol{d})_{\Gamma_d}, \\ &\qquad \forall\ \boldsymbol{u} \in \boldsymbol{H}^1(\Omega),\ p \in L^2(\Omega),\ \boldsymbol{\sigma} \in \boldsymbol{H}^{-1/2}(\Gamma_d),\ \boldsymbol{d} \in \boldsymbol{H}^{1/2}(\Gamma_d), \\ &\qquad \forall\ \boldsymbol{\lambda} \in \boldsymbol{V},\ \mu \in L^2(\Omega),\ \boldsymbol{\tau} \in \boldsymbol{H}^{-1/2}(\Gamma_d). \end{aligned} \tag{8.3}$$

Here $\boldsymbol{\lambda}, \mu, \boldsymbol{\tau}$ are the Lagrange multipliers for the state variables $\boldsymbol{u}, p, \boldsymbol{\sigma}$. By taking variations with respect to the Lagrange multipliers we obtain (8.2) augmented with $\boldsymbol{u}_d = \boldsymbol{d}$ on Γ_d. Taking variations with respect to the states $\boldsymbol{u}, p, \boldsymbol{\sigma}$ we obtain the weak form of the adjoint equations:

$$\begin{aligned} \nu a(\boldsymbol{\lambda}, \boldsymbol{v}) + c(\boldsymbol{v}, \boldsymbol{u}, \boldsymbol{\lambda}) + c(\boldsymbol{u}, \boldsymbol{v}, \boldsymbol{\lambda}) + b(\mu, \boldsymbol{v}) + (\boldsymbol{\tau}, \boldsymbol{v})_{\Gamma_d} &= -\nu a(\boldsymbol{u}, \boldsymbol{v})\ \forall\, \boldsymbol{v} \in \boldsymbol{V}, \\ b(q, \boldsymbol{\lambda}) &= 0 && \forall\, q \in L^2(\Omega) \\ (\boldsymbol{t}, \boldsymbol{\lambda})_{\Gamma_d} &= 0 && \forall\, \boldsymbol{t} \in \boldsymbol{H}^{-1/2}(\Gamma_d). \end{aligned} \tag{8.4}$$

Finally, by taking variations with respect to $\boldsymbol{d}$ we obtain the decision equation

$$\rho(\boldsymbol{d}, \boldsymbol{r})_{\Gamma_d} + (\boldsymbol{\tau}, \boldsymbol{r})_{\Gamma_d} = 0 \qquad \forall\, \boldsymbol{r} \in \boldsymbol{H}^{1/2}(\Gamma_d). \tag{8.5}$$

Equations (8.2), (8.4), (8.5) are the weak form of the first order optimality conditions for the optimal control problem. In [12], [13] there is extensive discussion on the existence of a solution and the existence of the Lagrange multipliers. Hou in his PhD thesis asserts the existence of a local minimum for the optimization problem and the existence of Lagrange multipliers that satisfy the first order optimality conditions. Furthermore, uniqueness is shown upon sufficiently small data. Note that in the absence of a Neumann condition ($\Gamma_N = \emptyset$) the space for the control variables needs to satisfy the incompressibility condition $(\boldsymbol{d} \cdot \boldsymbol{n})_{\Gamma_d} = 0$.

The strong form of the adjoint and decision equations can be obtained by using the following integration by parts formulas:

$$\begin{aligned} a(\boldsymbol{u}, \boldsymbol{v}) &= -(\boldsymbol{v}, \Delta \boldsymbol{u})_\Omega + ((\nabla \boldsymbol{u})\boldsymbol{n}, \boldsymbol{v})_\Gamma, \\ c(\boldsymbol{u}, \boldsymbol{v}, \boldsymbol{\lambda}) &= -c(\boldsymbol{u}, \boldsymbol{\lambda}, \boldsymbol{v}) - ((\nabla \cdot \boldsymbol{u})\boldsymbol{\lambda}, \boldsymbol{v})_\Omega + ((\boldsymbol{u} \cdot \boldsymbol{n})\boldsymbol{\lambda}, \boldsymbol{v})_\Gamma, \\ b(\mu, \boldsymbol{v}) &= (\nabla \mu, \boldsymbol{v})_\Omega - (\mu \boldsymbol{n}, \boldsymbol{v})_\Gamma. \end{aligned}$$

Upon sufficient smoothness we arrive at the strong form optimality conditions. Equation (8.1) is the strong form of the constraints. The strong form of the adjoint equations is given by

$$\begin{aligned} -\nu \nabla \cdot (\nabla \boldsymbol{\lambda} + \nabla \boldsymbol{\lambda}^T) + (\nabla \boldsymbol{u})^T \boldsymbol{\lambda} - (\nabla \boldsymbol{\lambda})\boldsymbol{u} + \nabla \mu &= \nu \nabla \cdot (\nabla \boldsymbol{u} + \nabla \boldsymbol{u}^T) \quad \text{in} \quad \Omega, \\ \nabla \cdot \boldsymbol{\lambda} &= 0 \quad \text{in} \quad \Omega, \\ \boldsymbol{\lambda} &= \boldsymbol{0} \quad \text{on} \quad \Gamma_u, \\ \boldsymbol{\lambda} &= \boldsymbol{0} \quad \text{on} \quad \Gamma_d, \\ -\mu \boldsymbol{n} + \nu(\nabla \boldsymbol{\lambda} + \nabla \boldsymbol{\lambda}^T)\boldsymbol{n} + (\boldsymbol{u} \cdot \boldsymbol{n})\boldsymbol{\lambda} &= -\nu(\nabla \boldsymbol{u} + \nabla \boldsymbol{u}^T)\boldsymbol{n} \quad \text{on} \quad \Gamma_N, \end{aligned} \tag{8.6}$$

and (equation for $\boldsymbol{\tau}$)

$$\nu(\nabla \boldsymbol{\lambda} + \nabla \boldsymbol{\lambda}^T)\boldsymbol{n} + \nu(\nabla \boldsymbol{u} + \nabla \boldsymbol{u}^T)\boldsymbol{n} - \boldsymbol{\tau} = \boldsymbol{0} \quad \text{on} \quad \Gamma_d. \tag{8.7}$$

We may also determine that the strong form of the decision equation is given by

$$\boldsymbol{\tau} = \rho \boldsymbol{d} \quad \text{on} \quad \Gamma_d. \tag{8.8}$$

In [12] estimates are given on the convergence rates of the finite element approximations to the exact solutions for the optimal control of steady viscous flow. For the case of boundary velocity control, the basic result is that, if the exact solutions are smooth enough, then, provided the Taylor-Hood element is used (for both adjoints and states), the solution error satisfies the following estimates:

$$\begin{aligned} \|\boldsymbol{u} - \boldsymbol{u}_h\|_0 &\leq \mathcal{O}(h^3), \\ \|p - p_h\|_0 &\leq \mathcal{O}(h^2), \\ \|\boldsymbol{\lambda} - \boldsymbol{\lambda}_h\|_0 &\leq \mathcal{O}(h^3), \\ \|\mu - \mu_h\|_0 &\leq \mathcal{O}(h^2). \end{aligned} \tag{8.9}$$

Here h is the maximum element size, and $\|\cdot\|_0$ is the $L^2(\Omega)$ norm.

9. Discrete and discretized optimality conditions.. In our implementation we have not discretized the continuous forms of the optimality conditions. Instead we have discretized the objective function and the Navier-Stokes equations and then we used this discretization to form the optimality conditions. In general discretization and differentiation (to obtain

optimality conditions) do not commute. That is, if $\boldsymbol{A}$ is the continuous (linearized) forward operator and $\boldsymbol{A}^*$ is its adjoint then in general

$$(\boldsymbol{A}^*)_h \neq (\boldsymbol{A}_h)^T.$$

We will show that for Galerkin approximation of the steady incompressible Navier-Stokes optimal control problem, discretization and differentiation do commute.

For the discretized equations we use the following notation:

$$\begin{aligned} a(\boldsymbol{u}_h, \boldsymbol{v}_h) + c(\boldsymbol{u}_h, \boldsymbol{u}_h, \boldsymbol{v}_h) &\dashrightarrow \mathbf{U}(\mathbf{u})\mathbf{u}, \\ a(\boldsymbol{u}_h, \boldsymbol{v}_h) + c(\boldsymbol{p}_h, \boldsymbol{u}_h, \boldsymbol{v}_h) + c(\boldsymbol{u}_h, \boldsymbol{p}_h, \boldsymbol{v}_h) &\dashrightarrow \mathbf{V}(\mathbf{u})\mathbf{p}, \\ a(\boldsymbol{u}_h, \boldsymbol{v}_h) &\dashrightarrow \mathbf{Q}\mathbf{u}, \\ b(q_h, \boldsymbol{u}_h) &\dashrightarrow \mathbf{P}\mathbf{u}, \\ (\boldsymbol{t}_h, \boldsymbol{u}_h)_{\Gamma_d} &\dashrightarrow \mathbf{T}\mathbf{u}, \\ (d_h, r_h)_{\Gamma_d} &\dashrightarrow \mathbf{M}\mathbf{d}. \end{aligned}$$

then, the discrete form for the Navier-Stokes equations is given by

$$\begin{aligned} \mathbf{U}(\mathbf{u})\mathbf{u} + \mathbf{P}^T\mathbf{p} + \mathbf{T}^T\boldsymbol{\sigma} &= \mathbf{f}_1, \\ \mathbf{P}\mathbf{u} &= \mathbf{f}_2, \\ \mathbf{T}\mathbf{u} &= \mathbf{T}\mathbf{d}. \end{aligned} \tag{9.1}$$

The discrete Lagrangian function is given by

$$\begin{aligned} \frac{1}{2}\mathbf{u}^T\mathbf{Q}\mathbf{u} + \frac{\rho}{2}\mathbf{d}^T\mathbf{M}\mathbf{d} + \boldsymbol{\lambda}^T\left\{\mathbf{U}(\mathbf{u})\mathbf{u} + \mathbf{P}^T\mathbf{p} + \mathbf{T}^T\boldsymbol{\sigma} - \mathbf{f}_1\right\} \\ + \boldsymbol{\mu}^T\left\{\mathbf{P}\mathbf{u} - \mathbf{f}_2\right\} + \boldsymbol{\tau}^T\left\{\mathbf{T}\mathbf{u} + \mathbf{T}\mathbf{d}\right\} = \mathbf{0}. \end{aligned} \tag{9.2}$$

By taking derivatives with respect to the discrete Lagrange multiplier vectors $\boldsymbol{\lambda}, \boldsymbol{\mu}, \boldsymbol{\tau}$, we recover the state equations (9.1). By taking derivatives with respect to the discrete state variables $\mathbf{u}, \mathbf{p}, \boldsymbol{\sigma}$, we obtain the discrete adjoint equations:

$$\begin{aligned} \mathbf{V}^T(\mathbf{u})\boldsymbol{\lambda} + \mathbf{P}^T\boldsymbol{\mu} + \mathbf{T}^T\tau &= -\mathbf{Q}\mathbf{u}, \\ \mathbf{P}\boldsymbol{\lambda} &= \mathbf{0}, \\ \mathbf{T}\boldsymbol{\lambda} &= \mathbf{0}. \end{aligned} \tag{9.3}$$

These equations correspond to the discretization of equations (8.4) provided that $\mathbf{V}^T\boldsymbol{\lambda}$ is the discretization of $a(\boldsymbol{\lambda}, \boldsymbol{u}) + c(\boldsymbol{v}, \boldsymbol{u}, \boldsymbol{\lambda}) + c(\boldsymbol{u}, \boldsymbol{v}, \boldsymbol{\lambda})$. The bilinear form $a(\cdot, \cdot)$ is symmetric so we omit it from our discussion. If ϕ denotes the basis function for $\boldsymbol{u}$, ψ_v for $\boldsymbol{v}$, and ψ_λ for $\boldsymbol{\lambda}$ then the (3×3)-block elements for the linearized state and the adjoint are:

$$\begin{aligned} \int_\Omega \mathbf{I}\,(\nabla\phi \cdot \boldsymbol{u})\psi_v + (\nabla\boldsymbol{u})\phi\psi_v \, d\Omega \qquad & \text{state element matrix}, \\ \int_\Omega \mathbf{I}\,(\nabla\psi_v \cdot \boldsymbol{u})\psi_\lambda + (\nabla\boldsymbol{u})^T\psi_\lambda\psi_v \, d\Omega \qquad & \text{adjoint element matrix}. \end{aligned}$$

Therefore, for a Galerkin formulation, the transpose of the discretized (linearized) state equations coincides with the discretization of the adjoint equations, i.e.

$$(\boldsymbol{A}^*)_h = (\boldsymbol{A}_h)^T.$$

One needs to be careful to use the weak form given by equation (8.4). If (8.6) were used without employing the reverse integration by parts on the term $c(\boldsymbol{u}, \boldsymbol{v}, \boldsymbol{\lambda})$, this would result in a discretization which is incompatible with the discrete optimization problem (which is what the optimizer sees). It would result in an unsymmetric KKT-matrix and possibly would prevent the optimizer from converging to a KKT point. A Petrov-Galerkin formulation would also be incompatible. Another important consequence of the compatibility between the discrete and the discretized optimality conditions is that one does not need to implement a separate adjoint solver.

In our formulation we do not solve explicitly for $\boldsymbol{\sigma}$ and $\boldsymbol{\tau}$. Upon sufficient smoothness of the tractions at the boundary, we can eliminate them. The resulting equations are equivalent to the formulations described in this section and the proofs for existence and uniqueness of a solution can be applied to the condensed system. We use a standard Galerkin approximation scheme (no upwinding) with Taylor-Hood elements to approximate the velocities and pressures and their adjoints.

We conclude this section with a note on continuation. To solve a Navier-Stokes control problem with large Reynolds number, some kind of continuation scheme is usually needed. We first solve a pure Stokes-flow optimal control problem ($Re_0 = 0$) and then we progressively increase the Reynolds number by $Re_{(+)} = Re + \Delta Re$. Along the lines of a predictor-corrector algorithm, one could set $\mathbf{u}_{(+)} = \mathbf{u} + (\partial_{Re})\mathbf{u}\Delta Re$, where $\partial_{Re}\mathbf{u}$ can be easily computed through a linearized forward solve. Since we consider only steady flows, we follow [8] and use fixed ΔRe, and simply set $\mathbf{u}_{(+)} = \mathbf{u}$, i.e. the initial guess at the new Reynolds number is the solution from the previous optimization step. Additionally, quasi-Newton information is carried forward to the next Reynolds number.

10. Finite element approximation error. In this section we use a model problem to verify the convergence rate estimates given in the previous section. We have constructed a solution to the Navier-Stokes equations[4] given by

$$\boldsymbol{u}^*(x, y, z) = \left\{1 - (x^2 + y^2)^2, x, -y\right\}^T,\ p^*(x, y, z) = x^2 + y^2 - z^2.$$

We restricted this solution to a cylindrical domain and we set part of its boundary to be the control domain Γ_d. The optimal control problem is of matching velocity type and the target velocity is $\boldsymbol{u}^*$. We defined the velocity boundary conditions on the circumferential walls to be the decision variables. On Γ/Γ_d we set $\boldsymbol{u} = \boldsymbol{u}^*$. The objective function is given by

$$\mathcal{J}(\boldsymbol{u}, \boldsymbol{u}_d, p) = \frac{1}{2}\int_\Omega (\boldsymbol{u}^* - \boldsymbol{u})^2\, d\Omega.$$

Since the boundary conditions for $\boldsymbol{u}, p$ on Γ/Γ_d are compatible with $(\boldsymbol{u}^*, p^*)$ the values for the objective function and the Lagrange multipliers at the minimum are zero.

Table 10.1 depicts the rates of convergence for the state variables and the Lagrange multipliers. The results are in good agreement with the theoretical predictions. The convergence rate for the velocities and their adjoints is approximately 2.92 (comparing errors between the first and second rows) and 2.96 (comparing errors between the second and third rows). For the pressures and their adjoints the convergence rate is 1.96 and 1.97, respectively.

[4]This is done as follows: First choose a vector-valued function $\boldsymbol{w}(\mathbf{x})$ in $\mathbb{R}^3$ and set $\boldsymbol{u}(\mathbf{x}) = \nabla\times\boldsymbol{w}(\mathbf{x})$. Then choose any scalar-valued function as the pressure field. The body force is then computed by the left-hand side of (8.1). Then the restriction of these functions to any (smooth enough) domain $\Omega \subset \mathbb{R}^3$ is a solution to the Navier-Stokes equations.

TABLE 10.1

*In this table the convergence rate of the finite element approximation towards an (*a priori*) known solution for a matching velocity problem is given. Here* **en** *is the number of elements; h is the cube root of the volume of the maximum inscribed sphere inside a tetrahedron of the finite element mesh. Near optimal convergent rates can be observed for the state and adjoint variables.*

en	h	$\|\boldsymbol{u}^* - \boldsymbol{u}_h\|_0$	$\|p_* - p_h\|_0$	$\|\boldsymbol{\lambda}_* - \boldsymbol{\lambda}_h\|_0$	$\|\mu_* - \mu_h\|_0$
124,639	0.80	1.34×10^{-4}	2.01×10^{-5}	3.88×10^{-4}	1.76×10^{-5}
298,305	0.53	0.41×10^{-4}	0.90×10^{-5}	1.19×10^{-4}	0.79×10^{-5}
586,133	0.40	0.17×10^{-4}	0.52×10^{-5}	0.50×10^{-4}	0.45×10^{-5}

11. Poiseuille flow. The Poiseuille flow is a solution of the Navier-Stokes equations[5], for a range of Reynolds numbers—as long we are in subcritical conditions. We have used the Poiseuille problem to study the efficiency of BFGS as a preconditioner.

A notable difference with the Stokes case is that a BFGS quasi-Newton update is used to precondition the reduced Hessian matrix. Since the problem is nonlinear, LNKS takes several iterations and quasi-Newton curvature information is built up. Quasi-Newton theory predicts that $\mathbf{B}_z$ approaches $\mathbf{W}_z$ as the iterates get closer to the solution. Therefore, one expects the effectiveness of the preconditioner to improve as the optimization algorithm progresses.

In the numerical experiments in this section, we do not make use of continuation to initiate the state and control variables. The reason is that our initial guess is always inside the basin of attraction of the solution. However, BFGS information is carried forward to the next Reynolds number, in both QN-RSQP and LNKS methods. To approximate the reduced Hessian (for preconditioning the KKT system in the Newton method and for driving the iterations in the quasi-Newton method), we invoke the limited-memory BFGS formula we described in Section 7.

TABLE 11.1

Algorithmic efficiency of the proposed preconditioners for a Poiseuille matching control problem. Recall that LNKS-I requires two linearized forward solves per iteration, whereas LINKS-II involves just application of the Schwarz approximation. The number of iterations for the KKT system is averaged across the optimization iterations. The problem has 21,000 state equations and 3,900 control variables; results are for 4 processors of the T3E-900. Time is in hours.

Re	**method**	**N/QN iter**	**KKT iter**	$\|\ \mathbf{g}_z\ \|$	**time**
100	QN-RSQP	262	—	1×10^{-4}	5.9
	LNK	3	186,000	9×10^{-6}	7.1
	LNKS-I	3	48	9×10^{-6}	3.2
	LNKS-II	3	4,200	9×10^{-6}	1.3
300	QN-RSQP	278	—	1×10^{-4}	6.4
	LNK	3	198,000	9×10^{-6}	7.6
	LNKS-I	3	40	9×10^{-6}	3.1
	LNKS-II	3	4,300	9×10^{-6}	1.4
500	QN-RSQP	289	—	1×10^{-4}	7.3
	LNK	3	213,000	9×10^{-6}	9.0
	LNKS-I	3	38	9×10^{-6}	3.0
	LNKS-II	3	4,410	9×10^{-6}	1.4

In the results presented in Table 11.1, the maximum number of BFGS vectors is 30. The

[5]Why was it not used as an exact solution for convergence rate estimates? The velocities are quadratic and since we are using quadratic elements the convergence is very fast (the solution is not exact due to integration errors).

forward problem preconditioner is given by Equation 4.5 (Part I). The Navier-Stokes discrete operator differs from the Stokes case: it is unsymmetric, so general QMR is used for the linearized Navier-Stokes solves. We found block-Jacobi to be very slow and instead opted for an overlapping additive Schwarz preconditioner with ILU(1) on each subdomain[6]. Results for a problem with 21,000 state and 3,900 design variables on 4 processors and for a sequence of three Reynolds numbers are presented in Table 11.1. Overall, one can observe that LNKS reduces significantly the execution time relative to QN-RSQP, just as in the Stokes problem.

The Navier-Stokes test problem provides an opportunity to improve the reduced Hessian preconditioner by building up quasi-Newton curvature information, something not possible for the Stokes flow problem, since a single KKT system is solved in that case. Although the test problems were not sufficiently nonlinear to require a large number of iterations, even with three Newton iterations we can already observe increasing effectiveness of the quasi-Newton approximation. This can be seen with LNKS-I as the number of KKT iterations drops with increasing Reynolds number.

As in the Stokes control problem, LNKS-II is faster than LNKS-I, since it avoids exact forward solves. The number of KKT iterations slightly increases with increasing Reynolds number, since the forward problem condition number deteriorates (recall that because of the inexact solves, the characteristics of the forward problem now affect the KKT system solution).

The outer solver performed very well requiring only 3 iterations to converge. In these problems we did not use inexact Newton's method with the KKT solves were fully converged at each iteration. No line search was used in the LNKS variants; we used the l_1-merit function for the QN-RSQP.

12. Flow around a cylinder. Unlike a quasi-Newton method that can insure a descent direction by a sufficiently accurate line search, there is no guarantee of descent and hence global convergence for the present Newton method. The problems studied so far were useful in verifying certain aspects of the theoretical results but they are only mildly nonlinear. In order to test LNKS further we study a highly nonlinear problem: that of flow around a cylinder.

The cylinder is anchored inside a rectangular duct, much like a wind tunnel. A quadratic velocity profile is used as an inflow Dirichlet condition and we prescribe a traction-free outflow. The decision variables are defined to be the velocities on the downstream portion of the cylinder surface.

Figures 12.1, 12.2 illustrate the optimization results for different Reynolds numbers. LNKS manages to completely eliminate the recirculation region in the downstream region of the cylinder. In order to avoid the suction controls we observed in the Stokes case, we imposed Dirichlet boundary conditions on the outflow of the domain. The incompressibility condition prevents the optimizer from driving the flow inside the cylinder[7].

Our experiments on the Stokes optimal control established the relation between the performance of the Krylov-Schur iteration and the forward problem preconditioner. Thus before we discuss results on the LNKS algorithm we give some representative results for the Navier-Stokes forward solver. We use an inexact Newton's method combined with the preconditioner we presented in Part I. A block-Jacobi ILU(0) preconditioner is used for the velocity block and as well as for the pressure mass matrix (scaled by $1/Re$); the latter is used to precondition

[6] For definitions of ILU(0) and ILU(1) see [19].

[7] In this case, our model—although mathematically correct—does not follow the physics very well. When Dirichlet conditions are specified everywhere on Γ, then $\int_\Gamma \boldsymbol{u} \cdot \boldsymbol{n}\, d\Gamma$ should add to 0. The constraint needs to be imposed explicitly, or with a proper function space. We do neither, but we increased the penalty parameter in the objective function.

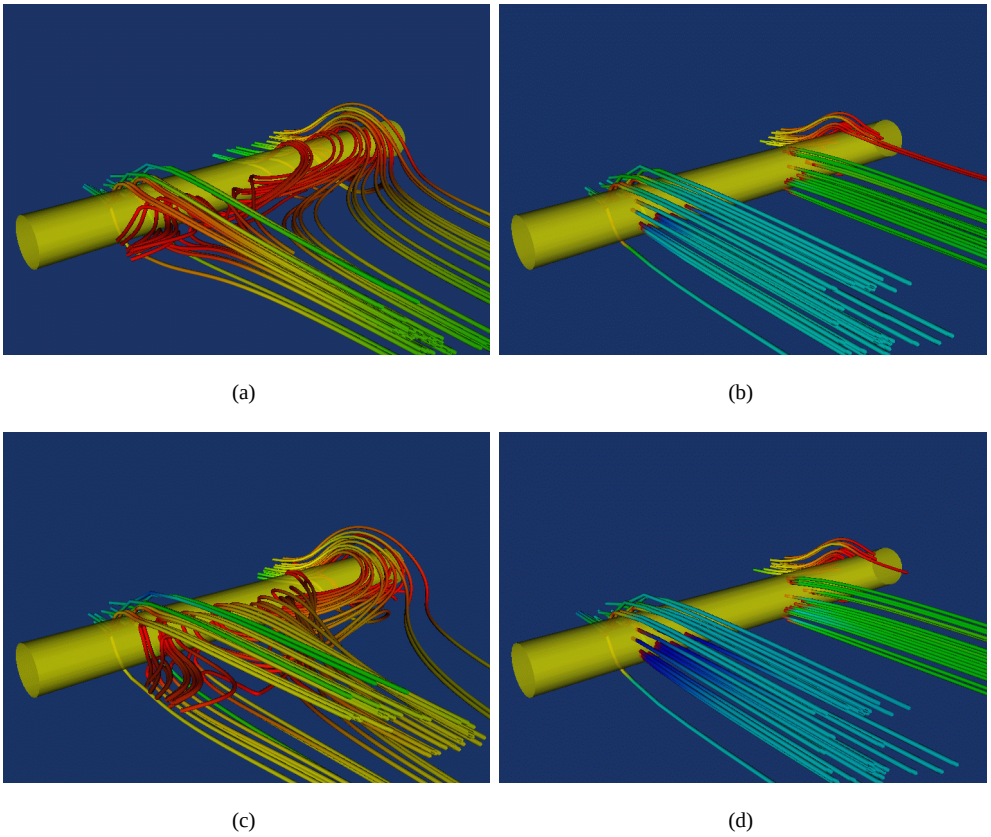

(a) (b)

(c) (d)

FIG. 12.1. *The top row depicts streamtubes of the flow for Reynolds number 20 and the bottom row for Reynolds number* 40. *The left column depicts the uncontrolled flow. The right column depicts the controlled flow.*

TABLE 12.1

Forward solver efficiency in relation to problem size and the Reynolds number for a 3D flow around a cylinder. ***(PEs)*** *is processor number;* ***(n)*** *is the problem size;* (Re) *is the Reynolds number;* ***(qmr)*** *is the number of aggregate Krylov iterations required to satisfy* $\|\boldsymbol{r}\|/\|\boldsymbol{r}_0\| \leq 1 \times 10^{-7}$*;* ***(nw)*** *is the number of Newton steps to satisfy* $\|\boldsymbol{c}\|/\|\boldsymbol{c}_0\| \leq 1 \times 10^{-6}$*; and* ***(t)*** *is time in seconds. The runs were performed on a T3E-900.*

		$Re = 20$			$Re = 30$			$Re = 60$		
PEs	**n**	**qmr**	**nw**	**t**	**qmr**	**nw**	**t**	**qmr**	**nw**	**t**
32	117.048	2,905	5	612	3,467	7	732	2,850	6	621
64	389,440	4,845	5	1,938	5,423	7	2,101	5,501	7	2,310
128	615,981	6,284	5	2,612	8,036	8	3,214	7,847	7	3,136

the pressure Schur complement block. We would very much like to use an ILU(1), as we did for the Poiseuille flow case, but memory limitations[8] prevented us from doing so.

Table 12.1 gives statistics for three different Reynolds numbers and for three different problem sizes. We report the (aggregate) number or Krylov iterations required to converge

[8] In our Navier-Stokes implementation, we store the state operator, the Hessian of the constraints and the Hessian of the objective. PSC's T3E-900 (where the majority of our runs took place), has only 128MB of memory per processor.

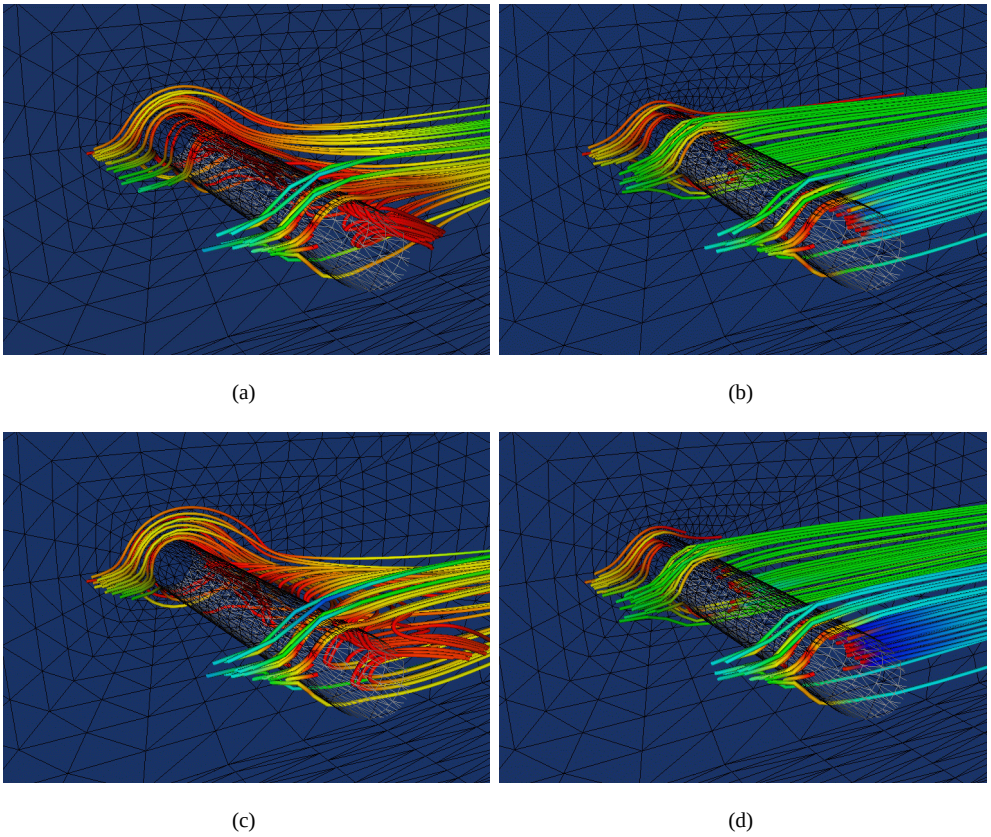

(a) (b)

(c) (d)

FIG. 12.2. *The top row depicts streamtubes of the flow for Reynolds number 20 and the bottom row for Reynolds number* 40. *The left column depicts the uncontrolled flow. The right column depicts the controlled flow.*

the Newton solver, the number of Newton iterations, and the total execution time. In these runs we used an inexact Newton's method but we did not use continuation. Comparing with Table 4.1 (Part I) we observe that the time for a forward solve has increased almost sixfold. However the time *per* iteration has remained on the same order compared to the Stokes case. For example, in the 128 processor problem and for Reynolds number 30, the average (Krylov) iteration count is 1005, whereas in the linear case it is 882. Similarly, the average time per Newton step is 401 seconds. The time for the Stokes solver is little higher, 421 seconds[9]. We can conclude that the forward solver performs reasonably well.

Let us return our discussion to the optimizer. Table 12.2 shows results for 32, 64, and 128 processors of a T3E-900 for a roughly doubling of problem size. Results for two different preconditioning variants of LNKS are presented: the exact (LNKS-I) and inexact (LNKS-II) version of the Schur preconditioner. The globalized LNKS algorithm is compared with QN-RSQP. In LNKS-II-TR we activate the inexact Newton method. Continuation was used for the initial guess at Reynolds number 60 by using the solution from Reynolds number 30 as the initial guess. The reduced Hessian preconditioner is a combination of the BFGS and

[9]The reason is somewhat esoteric; it has to do with the scaling between the velocity and pressure block of the forward problem. Increasing the Reynolds number improves this scaling and thus improves the eigenvalue distribution. Of course this is true up to certain Reynolds number. For higher values the Jacobian becomes highly unsymmetric and ill-conditioned.

TABLE 12.2

*The table shows results for 32, 64, and 128 processors of a Cray T3E for a roughly doubling of problem size. Results for the QN-RSQP and LNKS algorithms are presented. (***QN-RSQP***) is quasi-Newton reduced-space SQP; (***LNKS-I***) requires two exact solves per Krylov step combined with 2-step-stationary-BFGS preconditioner for the reduced Hessian; in (***LNKS-II***) the exact solves have been replaced by approximate solves; (***LNKS-II-TR***) uses a truncated Newton method and avoids fully converging the KKT system for iterates that are far from a solution. (***time***) is wall-clock time in hours on a T3E-900. Continuation was used only for* $Re = 60$.

$Re = 30$

states controls	method	N or QN iter	KKT iter	time
117,048	QN-RSQP	161	—	32.1
2,925	LNKS-I	5	18	22,8
(32 procs)	LNKS-II	6	1,367	5,7
	LNKS-II-TR	11	163	1.4
389,440	QN-RSQP	189	—	46.3
6,549	LNKS-I	6	19	27.4
(64 procs)	LNKS-II	6	2,153	15.7
	LNKS-II-TR	13	238	3.8
615,981	QN-RSQP	204	—	53.1
8,901	LNKS-I	7	20	33.8
(128 procs)	LNKS-II	6	3,583	16.8
	LNKS-II-TR	12	379	4.1

$Re = 60$

states controls	preconditioning	Newton iter	average KKT iter	time (hours)
117,048	QN-RSQP	168	—	33.4
2,925	LNKS-I	6	20	31,7
(32 procs)	LNKS-II	7	1,391	6,8
	LNKS-II-TR	11	169	1.5
389,440	QN-RSQP	194	—	49.1
6,549	LNKS-I	8	21	44.2
(64 procs)	LNKS-II	7	2,228	18.9
	LNKS-II-TR	15	256	4.8
615,981	QN-RSQP	211	—	57.3
8,901	LNKS-I	8	22	45.8
(128 procs)	LNKS-II	8	3,610	13.5
	LNKS-II-TR	16	383	5.1

2-step preconditioners (as we described in Section 7). For the line search algorithm we use the augmented Lagrangian merit function.

In this problem, QN-RSQP managed to converge, but only after 48 hours. LNKS-I, although faster, does not reduce the required time significantly. LNKS-II does better—4 to 5 times faster than QN-RSQP.

The most notable finding in Table 12.2 is the dramatic acceleration of the LNKS algorithm which is achieved by using LNKS-II-TR—the inexact version of the Newton method. The inexactness did not interfere at any point with the merit function and in all cases we observed quadratic convergence. For both Reynolds number 30 and 60 LNKS-II-TR runs more than 10 times faster than QN-RSQP. This is in agreement with the performance improvements we observed with the Stokes equations.

Undoubtedly the external cylinder flow problem is highly nonlinear. The augmented Lagrangian globalization performed robustly and we did not have problems converging the equations. Not once did the QN-RSQP safeguard get activated—triggered from a negative curvature direction. Finally, it is worth noting that an optimum is found at a cost of 5 to 6

flow simulations—remarkable considering that there are thousands of control variables.

13. Flow around a Boeing 707 wing. To further test LNKS we studied the optimal control of a flow around a Boeing 707 wing. In this problem the control variables are the velocities (Dirichlet conditions) on the downstream half of the wing. The Reynolds number (based on the length of the root of the wing) was varied from 100 to 500 and the angle of attack was fixed at 12.5 degrees. The problem size in this example is 710,023 state variables and 4,984 control variables.

Table 13.1 summarize the results from this set of experiments. The main purpose of this analysis is to compare the continuation idea with the other globalization heuristics. In addition we employ the double inexactness trick, that is, we solve inexactly in both the continuation loop and the Lagrange-Newton loop. Several observations are in place. It is apparent

TABLE 13.1

*In this table we present results for the wing flow test case. The size of this problem is 710,023 state and 4,984 decision variables. The runs were performed on 128 processors on a T3E-900. Here (Re) is the Reynolds number; (***iter***) is the aggregate number of Lagrange-Newton iterations—the number in parenthesis is the number of iteration in the last step; (***time***) is the overall time in hours; (***qn***) is the number of QN-RSQP steps—the number in parenthesis gives how many times a negative curvature was detected; (***minc***) is the number of non-monotone line search iterations—in parenthesis is the number of times this heuristic failed. The globalized LNKS-II-TR algorithm is used. The Lagrange-Newton solver was stopped after 50 iterations. In the last column ($Re \times \Delta f$) gives the reduction of the objective function (with the respect the uncontrolled flow). "no cont" means that continuation was not activated.*

Re	**iter**	**time**	**qn**	**minc**	$\|\mathbf{g} + \mathbf{A}^T\boldsymbol{\lambda}\|$	$\|\mathbf{c}\|$	$Re \times \Delta f$
100 no cont	19	4.06	2	4	9×10^{-6}	9×10^{-6}	4.065
cont							
200 no cont	39	7.8	6(1)	2	9×10^{-6}	9×10^{-6}	5.804
cont	20(10)	4.6	0	3	9×10^{-6}	9×10^{-6}	5.805
300 no cont	48	11.8	16(3)	0	9×10^{-6}	9×10^{-6}	6.012
cont	29(11)	6.4	0	2	9×10^{-6}	9×10^{-6}	6.016
400 no cont	50	13.6	40(3)	0	2×10^{-4}	3×10^{-3}	3.023
cont	33(11)	7.36	0	6(1)	9×10^{-6}	9×10^{-6}	8.345
500 no cont	50	16.7	42(5)	0	4×10^{-2}	9×10^{-2}	1.235
cont	39(14)	9.09	1	5(1)	9×10^{-6}	9×10^{-6}	10.234

that in this problem continuation is crucial. For Reynolds numbers larger than 300, LNKS was forced to early termination (we set the Lagrange-Newton iteration bound to 50). In the last row ($Re = 500$) and when we did not use continuation, LNKS ends up switching to a QN-RSQP step 42 times out of a total of 50 iterations; 5 times a negative curvature direction was detected. As a result LNKS was terminated without having reached the convergence criteria. Furthermore, the small reduction in the objective function and the residuals (last three columns) indicate there was little progress at each optimization step. Note that in these examples we did not activate backtracking in the continuation parameter.

It could be argued that a reason the algorithm stagnated was the early termination of the Krylov-Schur solver—because of the inexactness. We did not conduct exhaustive experiments to confirm or reject this claim. However, our experience on numerous problems suggests that it is the ill-conditioning and nonlinearity of these problems that leads to stagnation and not the inexactness. In our tests (systematic or during debugging and development) it was never the case that a run with exact solves converged in reasonable time, and the inexact version did not. On the contrary, inexactness significantly reduced execution times.

On the other hand, when we used continuation (fairly large steps on the Reynolds number), the algorithm successfully converged after 39 Lagrange-Newton iterations. It required switching to QN-RSQP just once. In the fifth column we monitor the non-monotone line

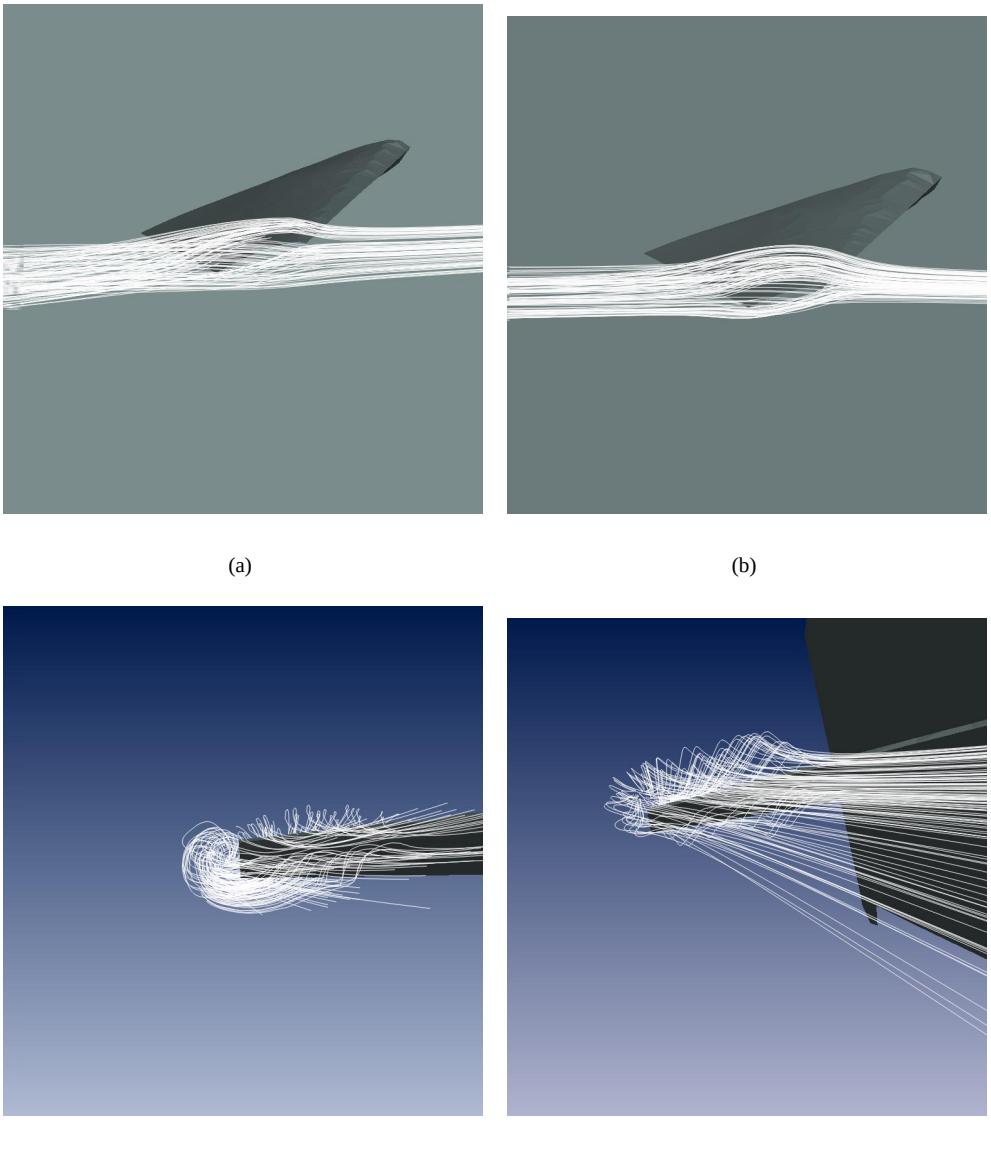

(a) (b)

(c) (d)

FIG. 13.1. *The left column depicts streamlines of the uncontrolled flow. The right column depicts streamlines of the controlled flow. Top row gives a side snapshot of the flow; bottom row gives a front view. The Reynolds number (based on the length the root of the wing) is 500.*

search criterion. Recall that if the merit function line search on the LNKS step fails, we perform a line search with a different merit—the KKT residual (i.e. the first order optimality conditions). If the step gets accepted, via backtracking, we use it as an update direction. Eventually, we insist that the (augmented Lagrangian) merit gets reduced. This strategy was very successful 20 times and it failed only twice[10].

[10]In general, using the residual of the KKT conditions to test a step can compromise robustness since the opti-

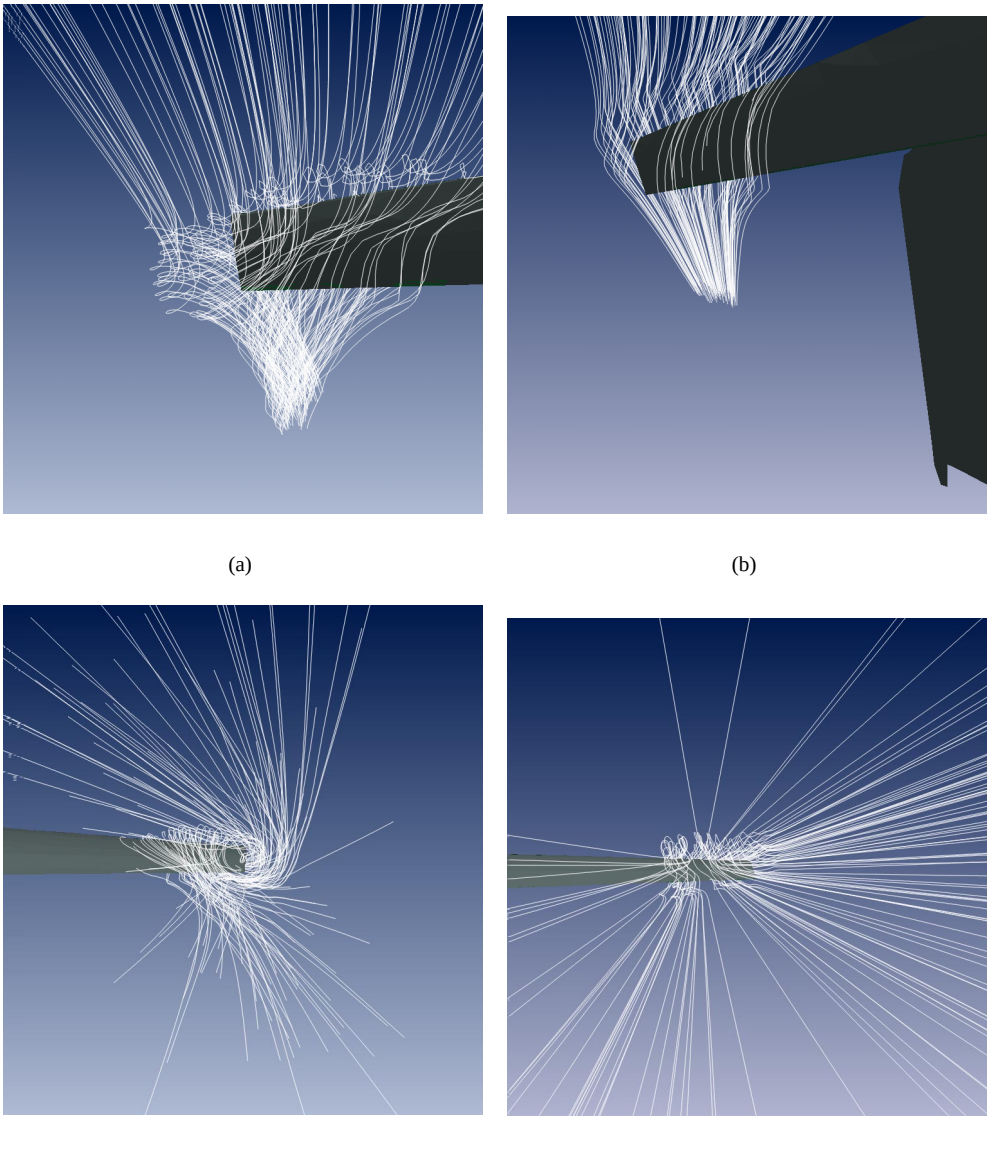

FIG. 13.2. *The left column depicts streamlines of the uncontrolled flow. The right column depicts streamlines of the controlled flow. Top row gives a snapshot of the flow from below; bottom row gives a back view. Reynolds number is 500.*

Finally we conclude with some comments on the physics of this problem. Figure 13.1, 13.2 depicts snapshots of the uncontrolled and controlled flow for Reynolds number 500. The wing-tip vortices are eliminated by the optimizer. But at what cost? Figure 13.3 shows a snapshot of the (scaled up control variables—the velocity boundary conditions. It is obvious that the optimizer designed a perforated wing, which means a significant reduction in lift.

mizer could get trapped to a saddle point or a local maximum.

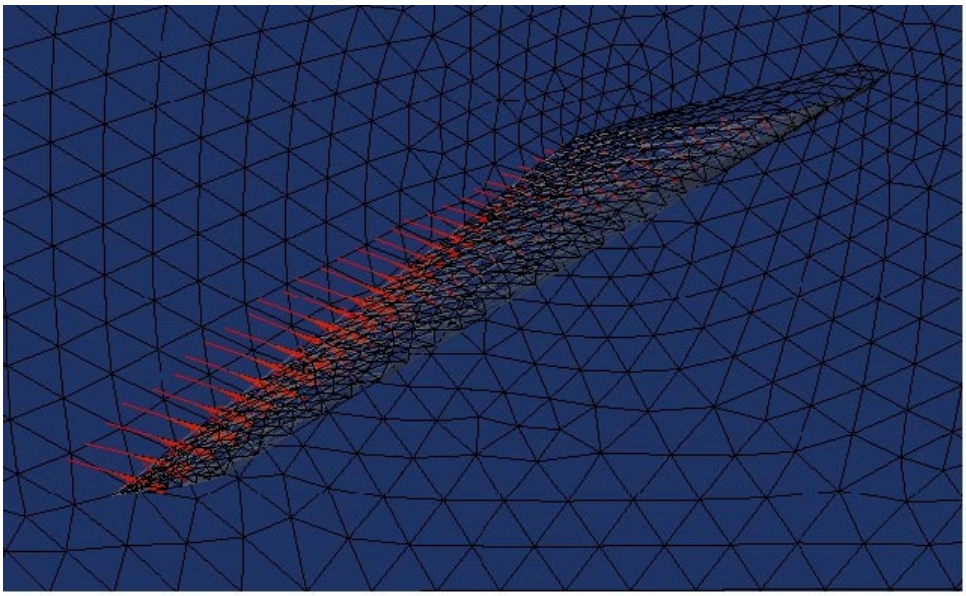

FIG. 13.3. *Snapshot of the (Dirichlet control) velocity field on the wing.*

This plane may never leave the ground!

14. Conclusions. In the second part of the paper we studied the application of the LNKS method to a set of different optimal flow control problems. Our tests confirm that LNKS is a robust and scalable algorithm for PDE-constrained optimization. The Krylov-Schur preconditioner maintained and even increased (due to BFGS) its effectiveness, and the Lagrange-Newton method exhibited the well known mesh-independence convergence properties. Inexact Newton steps dramatically accelerated the algorithm and continuation ensured global convergence.

The results reveal at least an order of magnitude improvement in time over popular quasi-Newton methods, rendering tractable some problems that were out of reach previously. Indeed, the optimum is often found in a *small* multiple of the cost of a single simulation.

We believe that the LNKS method is a very powerful tool. For this reason we decided to direct effort at developing a code that will be usable by the scientific community. In a forthcoming paper we will discuss *Veltisto*, a package for large-scale, PDE-constrained optimization on parallel computers.

Acknowledgments. We thank Satish Balay, Bill Gropp, Lois McInnes, and Barry Smith of Argonne National Lab for their work in making PETSc available to the research community. We also thank Jonathan Shewchuk of UC Berkeley for providing the meshing and partitioning routines Pyramid and Slice, and David Marcum of Mississippi State for providing the meshing module AFLR. Finally, we thank David Keyes of ICASE/Old Dominion University, David Young of Boeing, and the other members of the TAOS project—Roscoe Bartlett, Larry Biegler, Greg Itle, Ivan Malčević, and Andreas Wächter—for their useful comments.

REFERENCES

[1] I. BABUŠKA, *The finite element method with lagrangian multipliers*, Numerische Mathematik, 20 (1973), pp. 179–192.

[2] P. T. BOGGS AND J. W. TOLLE, *A strategy for global convergence in a sequential quadratic programming algorithm*, SIAM Journal on Numerical Analysis, 26 (1989), pp. 600–623.
[3] J. DENNIS E., JR., M. EL-ALEM, AND M. C. MAGIEL, *A global convergence theory for general trust-region-based algorithms for equality constrained optimization*, SIAM Journal on Optimization, 7 (1997), pp. 177–207.
[4] S. C. EISENSTAT AND H. F. WALKER, *Globally convergent inexact Newton methods*, SIAM Journal on Optimization, 4 (1994), pp. 393–422.
[5] ———, *Choosing the forcing terms in an inexact Newton method*, SIAM Journal on Scientific Computing, 17 (1996), pp. 16–32.
[6] R. FLETCHER, *Practical Methods of Optimization*, John Wiley and Sons, second ed., 1987.
[7] P. E. GILL, W. MURRAY, AND M. H. WRIGHT, *Practical Optimization*, Academic Press, 1981.
[8] M. D. GUNZBURGER, *Finite Element for Viscous Incompressible Flows*, Academic Press, 1989.
[9] M. D. GUNZBURGER, ed., *Flow Control*, vol. 68 of IMA Math. Appl., Springer-Verlag, New York, 1995.
[10] M. D. GUNZBURGER AND R. A. NICOLAIDES, eds., *Incompressible Computational Fluid Dynamics*, Cambridge University Press, 1993.
[11] M. HEINKENSCHLOSS AND L. N. VICENTE, *Analysis of inexact trust-region SQP algorithms*, Tech. Rep. TR99-18, Rice University, Department of Computational and Applied Mathematics, 1999.
[12] L. S. HOU, *Analysis and Finite Element Approximation of some Optimal Control Problems Associated with the Navier-Stokes Equations*, PhD thesis, Carnegie Mellon University, Department of Mathematical Sciences, Pittsburgh, August 1989.
[13] L. S. HOU AND S. S. RAVINDRAN, *Numerical approximation of optimal flow control problems by a penalty method: Error estimates and numerical results*, SIAM Journal on Scientific Computing, 20 (1999), pp. 1753–1777.
[14] C. KELLEY AND E. W. SACHS, *Truncated Newton methods for optimization with inaccurate functions and gradients*, SIAM Journal on Optimization, 10 (1999), pp. 43–55.
[15] C. T. KELLEY AND D. E. KEYES, *Convergence analysis of pseudo-transient continuation*, SIAM Journal on Numerical Analysis, 35 (1998), pp. 508–523.
[16] F. LEIBRITZ AND E. W. SACHS, *Inexact SQP interior point methods and large scale optimal control problems*, SIAM Journal on Control and Optimization, 38 (1999), pp. 272–293.
[17] S. G. NASH AND A. SOFER, *Linear and Nonlinear Programming*, McGraw-Hill, 1996.
[18] J. NOCEDAL AND S. J. WRIGHT, *Numerical Optimization*, Springer, 1999.
[19] Y. SAAD, *Iterative Methods for Sparse Linear Systems*, PWS Publishing Company, 1996.
[20] K. SCHITTKOWSKI, *The nonlinear programming method of wilson, han, and powell with an augmented Lagrangian type line search function*, Numerische Mathematik, 38 (1981), pp. 83–114.
[21] T. STEIHAUG, *The conjugate gradient method and trust regions in large scale optimization*, SIAM Journal on Numerical Analysis, 20 (1983), pp. 626–637.
[22] H. YAMASHITA, *A globally convergent constrained quasi-Newton method with an augmented Lagrangian type penalty function*, Mathematical Programming, 23 (1982), pp. 75–86.

This research was in part sponsored by National Science Foundation (NSF) grant no. CCR-0122581.